Neutron scattering study of the lattice dynamics of Cr_3Si

J.-E. Jørgensen,* J. D. Axe, L. M. Corliss, and J. M. Hastings
Brookhaven National Laboratory, Upton, New York 11973
(Received 21 December 1981)

Phonons with wave vectors along [100], [110], and [111] directions and energies $\lesssim 36$ meV were measured in a large (1.2 cm^3) single crystal using triple-axis spectroscopy. Scattering intensities were used to make symmetry assignments for the $\vec{q}=0$ modes. A total of 15 of the expected 24 $\vec{q}=0$ modes are identified and show much accidental near-degeneracy. The Γ'_{25} mode frequency is in agreement with Raman results. A short-ranged central-force Born–von Karman model is constructed and used to discuss the results.

I. INTRODUCTION

The understanding of the interrelationships that exist between superconductivity, structural phase transformations, and lattice dynamics is nowhere more critical than for materials with the β-tungsten ($A15$) structure. Many high-temperature superconductors are to be found among the intermetallic compounds with this structure. Many of these same materials either undergo phase transformations driven by soft acoustic phonons (V_3Si and Nb_3Sn are the best studied examples) or elastic softness that indicates a tendency toward such an instability. However, in spite of nearly two decades of discussion and theorizing, we are far from a precise understanding of the role of the structural instabilities on the superconducting properties.[1]

Part of the difficulty is that very little is reliably known about the phonons, and consequently the interatomic forces, in the $A15$ metals. While inelastic neutron scattering can, in principle, provide such information, such studies[2,3] as have been possible have been limited to low-lying acoustic phonons (because of sample size requirements necessary to extend the studies to higher phonon energies) or to density-of-states studies.[4] Recently, Raman scattering measurements[5,6] have given some valuable information on certain of the long-wavelength optic modes, but due to the relative complexity of the $A15$ structure, much more information is necessary before a picture of the interatomic forces will emerge.

Cr_3Si is an unexciting member of the glamorous $A15$ family. It has no superconducting transition down to 0.015 K (Ref. 7) and neutron powder diffraction at 6 K shows that Cr_3Si remains cubic at low temperatures.[8] However, rather large single crystals can be grown (unlike Nb_3Sn) and both Cr and Si have favorable neutron scattering properties (unlike V_3Si). We therefore felt it was worthwhile to measure and classify as much as possible of the Cr_3Si phonon spectrum by inelastic neutron scattering. While of some intrinsic interest, our findings will become more important when comparable data become available in one or more high-T_c $A15$ compounds.

In Sec. II we describe the sample, the measurements, and the experimental results. In Sec. III we describe and apply to our results some considerations of the intensities of the $q=0$ phonon modes. These relations follow from symmetry arguments alone and furnish model independent tools for making the mode assignments. We believe that these relations will be a useful and possibly necessary component in the understanding of inelastic neutron scattering data on other $A15$ materials as they become available. In Sec. IV we make a preliminary attempt to relate our observations to a model with short-ranged interatomic forces and make some final observations and comments.

II. EXPERIMENTAL DATA

The measurements were performed using a single crystal with a volume of ~ 1.2 cm^3. The crystal was grown using the zone-melting technique.[9] The measurements were performed using triple-axis spectrometers at the Brookhaven High Flux Beam Reactor (HFBR). Most data were collected with the spectrometer in the constant-Q mode of operation. The analyzer was (002) pyrolytic graphite (PG). The monochromator was PG(002) or Be(002) depending upon the (fixed) incident neutron energy. Most measurements were made in the (hkk) scattering zone.

Dispersion curves were measured at 295 K in the [100], [110], and [111] directions. The data are tabulated in Table I and plotted in Fig. 1. We believe the data to be reasonably complete in the 0–30-meV range, although, as will become clear, there is evidence for a number of nearly degenerate branches which remain unresolved. In addition, measurements of the accessible long-wavelength acoustic modes were repeated at 77 K. No substantial temperature variation was observed.

TABLE I. Measured phonon energies (in meV) of Cr_3Si along the [100], [110], and [111] symmetry directions at room temperature.

ξ	TA	LA	Optic modes
$\vec{q}=0$			26.0, 33.0
$\vec{q}=(\xi,\xi,\xi)$	(Λ direction)		
0.030	2.25		
0.050	3.85		
0.068		9.0	
0.070	5.25		
0.100	7.50	12.0	25.5, 25.8, 33.0
0.122		15.0	
0.154		18.0	
0.182		21.0	
0.200	14.80		24.9, 27.3, 31.0
0.212		24.0	
0.254			
0.300	20.80	25.0	28.2
0.310			30.0
0.400	24.80	26.0	28.0, 30.0, 36.0
0.500	27.50		32.5
$\vec{q}=(\xi,0,0)$	(Δ direction)		
0.090		9.0	
0.100			25.5, 26.5
0.150		12.0	
0.195		15.0	
0.200	8.3		24.2, 25.9, 26.6
0.245		18.0	
0.300	12.0	21.0	23.0, 25.6, 26.9
0.360		24.0	
0.400	15.5		21.2, 26.1
0.435		27.0	
0.500	18.5	29.0	27.0
$\vec{q}=(\xi,\xi,0)$	(Σ direction)		
0.030	1.75		
0.040	2.35		
0.046		9.0	
0.050	3.10		
0.070	4.10		
0.080	4.57		
0.100			25.4, 26.0
0.110		12.0	
0.146		15.0	
0.150	8.40		
0.188		18.0	
0.200			25.0, 27.0
0.221		21.0	
0.266		24.0	
0.300	16.00		24.0, 28.5
0.350	18.30		
0.400	20.05	26.5	23.0
0.450	21.90		
0.500	22.40		

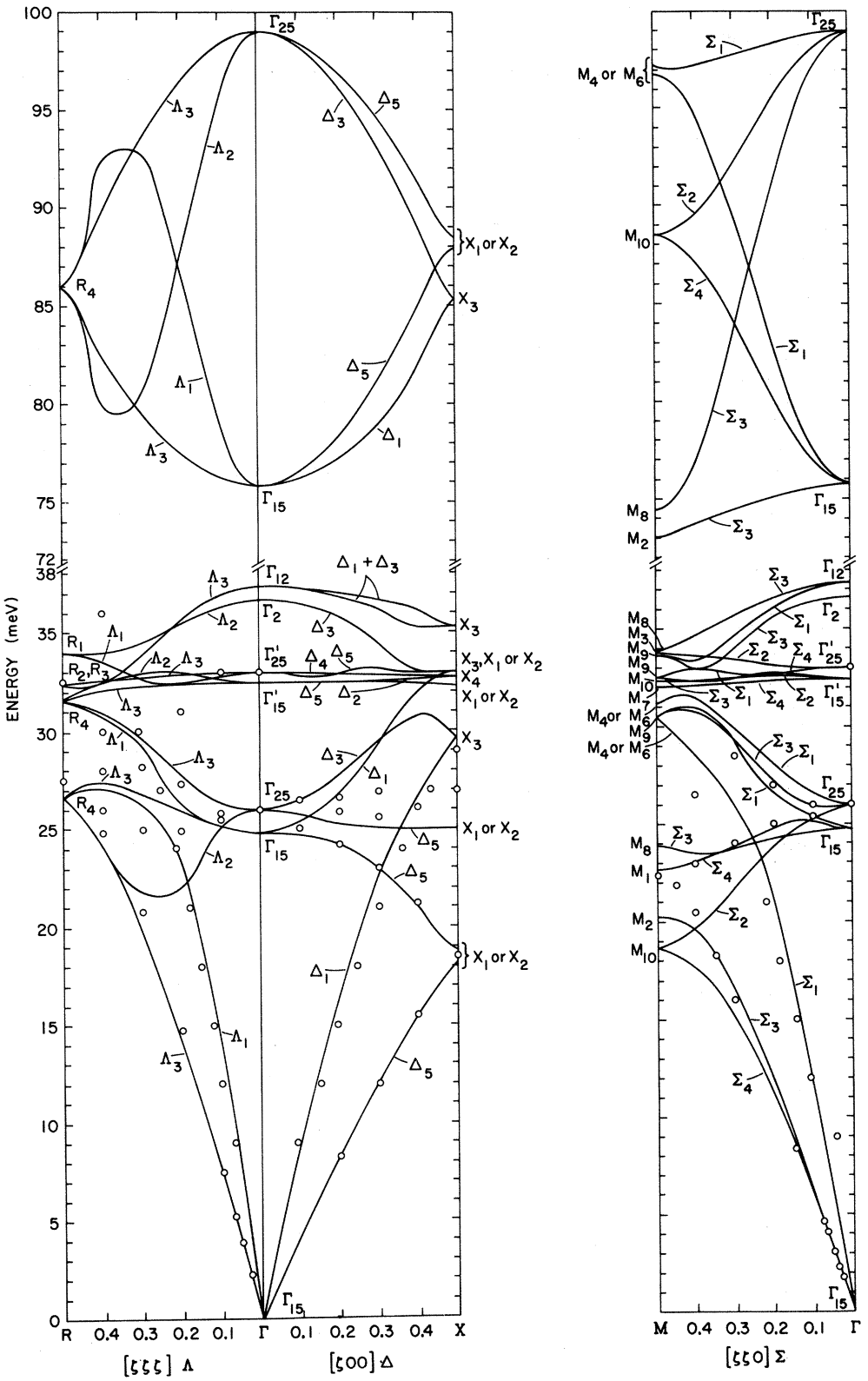

FIG. 1. Phonon dispersion in Cr_3Si. The circles represent measured data points. The lines are the result of the model calculation, as are the mode assignments except at $q = 0$.

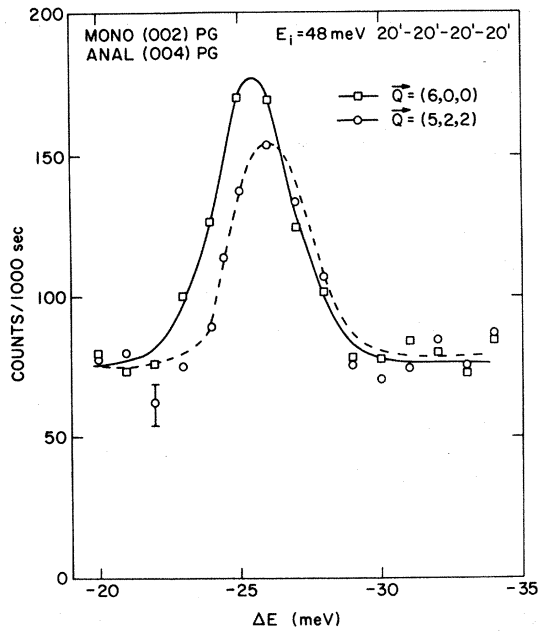

FIG. 2. Examples of $q=0$ phonon groups.

Two sets of data more or less representative of the majority of the strong optic phonons are shown in Fig. 2. The fact that a strong response at $\Delta E=26$ meV was seen both at $\vec{Q}=(5,2,2)$ and (6,0,0) is an important constraint on the $q=0$ mode assignments, as will be shown in Sec. III, where mode intensities are considered in some detail. In this and a few other critical cases, to reduce the possibility of spurious and multiple scattering processes the measurements were repeated at several different neutron energies, at different angles of rotation about the scattering vector, and in both energy-loss and energy-gain modes.

III. MODE ASSIGNMENTS

The experimental data of Table I are of very limited utility without some additional information concerning the classification of the modes. For example, any attempt to compare the data with model calculations is, in practice, hopeless without such information. Fortunately, such information can often be deduced from a study of the intensity variation of inelastic neutron scattering with momentum transfer, $\vec{Q}$, for the same phonon group, i.e., one varies $\vec{Q}$, while holding $\vec{q}=\vec{Q}-\vec{G}$ constant, where $\vec{G}$ is any reciprocal-lattice vector. The basis of this procedure is that the phonon intensities are proportional to the square of an inelastic structure factor,

$$F_j(\vec{q},\vec{Q})=\sum_\kappa b_\kappa m_\kappa^{-1/2}[(\vec{Q}\cdot\vec{e}_\kappa(\vec{q},j)] \times\exp(i\vec{Q}\cdot\vec{r}_\kappa)\exp[-W_\kappa(Q)]\ , \quad (1)$$

where the phonon is characterized by a wave vector $\vec{q}$ and branch index j, and κ labels the atoms in the unit cell. $W_\kappa(\vec{Q})$, $\vec{e}_\kappa(\vec{q},j)$, b_κ, $\vec{r}_\kappa$, and m_κ are Debye-Waller factor, polarization vector, scattering length, position vector, and mass of atom κ. $\vec{Q}$ is the scattering vector. Use of Eq. (1) for a group theoretical classification of the observed modes requires a knowledge of the phonon eigenvectors $\vec{e}(\vec{q},j)$.

A group theoretical analysis of the phonon modes in the $A15$ structure has been given by Achar and Barsch.[9] Corresponding to the eight atoms/unit cell, there are 24 phonon branches which show considerable degeneracy at high-symmetry points in the Brillouin zone. For example, at the R point $[\vec{q}=(\frac{1}{2},\frac{1}{2},\frac{1}{2})]$ the modes are distributed among four symmetry representations as follows:

$$R_1(2)+R_2(2)+R_3(2)+3R_4(6),\quad \vec{q}=(\tfrac{1}{2},\tfrac{1}{2},\tfrac{1}{2})\ ,$$

where $mR_i(n)$ indicates that the n-fold degenerate representation R_i occurs m times. Similarly, for $\vec{q}=0$ (Γ point) the decomposition is

$$\Gamma_2(1)+\Gamma_{12}(2)+\Gamma'_{15}(3)+\Gamma'_{25}(3) +2\Gamma_{25}(3)+3\Gamma_{15}(3),\quad q=0\ .$$

R and Γ are the points of highest symmetry.

Achar and Barsch[10] also construct from Cartesian displacements of the atoms a set of basis functions with irreducible symmetry properties. In the event that the phonons of a given symmetry occur only once (e.g., Γ_2, Γ_{12}, Γ'_{15}, and Γ'_{25}) these symmetry basis functions are also the phonon eigenvectors. If there are m phonon modes of a particular representation, there are m linearly independent basis sets and the phonon eigenvectors are some appropriate linear combination of them. Since both the basis vectors and eigenvectors are orthonormal sets, for the case of Γ_{25} for which $m=2$

$$\begin{pmatrix}\vec{e}_1\\ \vec{e}_2\end{pmatrix}=\begin{pmatrix}\cos\phi & \sin\phi\\ -\sin\phi & \cos\phi\end{pmatrix}\begin{pmatrix}\vec{s}_1\\ \vec{s}_2\end{pmatrix}\ \Gamma_{25}\text{ modes}\ , \quad (2)$$

where $(\vec{e}_1,\vec{e}_2)$ and $(\vec{s}_1,\vec{s}_2)$ are the two-component eigenvector and symmetry basis sets of the repeated representation, and ϕ is a parameter which is fixed not by symmetry but by details of the interatomic forces as expressed in the dynamical matrix, $D(\vec{q}=0)$.

For Γ_{15}, $m=3$ and the situation would be more complicated except for the fact that one of the Γ_{15} modes represents uniform translations ($\vec{q}=0$ acoustic modes). If the remaining symmetry basis functions (s'_1,s'_2) are chosen orthogonal to the Γ_{15} acoustic mode, one again finds

$$\begin{pmatrix}\vec{e}_1\\ \vec{e}_2\end{pmatrix}=\begin{pmatrix}\cos\theta & \sin\theta\\ -\sin\theta & \cos\theta\end{pmatrix}\begin{pmatrix}\vec{s}'_1\\ \vec{s}'_2\end{pmatrix}\ \Gamma_{15}\text{ modes}\ . \quad (3)$$

In summary, the $q=0$ eigenvectors and thus the inelastic structure factors can be characterized uniquely by symmetry except for the Γ_{25} and Γ_{15} modes which require the specification of individual mixing angles which can be treated as unknown empirical parameters in order to compare intensities calculated using Eq. (1) with experiment. When this is done, a number of "selection rules" are found, the most general of which are as follows:

$$\text{For } \Gamma_i=\Gamma_2,\ \Gamma_{12},\ \Gamma'_{15},\ \Gamma'_{25}\ ,\quad I_{\Gamma_i}(hkl)=0,\ (h,\ k,\ l) \text{ all even}\ ; \tag{4a}$$

$$\text{for } \Gamma_i=\Gamma_{15}\ ,\quad I_{\Gamma_{15}}(hkl)=0,\ (h,\ k,\ l) \text{ all odd}\ , \tag{4b}$$

where h, k, l are Miller indices. However, some essential information is revealed only by numerical analysis, as discussed below.

We restrict our detailed description of intensity considerations to the $\vec{q}=0$ phonon group seen at 26 meV. Figure 3 shows the relative intensity of this phonon group at 22 different reciprocal-lattice positions. The absence of a bar indicates that the intensity was less than $\frac{1}{3}$ of the lowest observation recorded on the figure. The presence of intensity at (600) and (066), together with Eq. (4a), eliminates all but Γ_{15} and Γ_{25} modes. Strong (733), (555), and (533) intensity together with (4b) would seem to resolve the issue in favor of Γ_{25}. However, a detailed comparison of the data with predictions of Eqs. (1) and (2) produced no satisfactory result for any value of ϕ. [In fact, $I(600)=0$, identically, for Γ_{25} modes.]

This apparent contradiction was resolved only with the realization that preliminary model calculations, to be described in Sec. IV, showed for a wide range of forces constants that the lowest $\vec{q}=0$ optic mode was sometimes Γ_{15}, sometimes Γ_{25}, but with little separation in energy. This led to a fresh attempt to understand the intensities of the 26-meV group by adding both Γ_{15} and Γ_{25} intensities and adjusting both mixing angles θ and ϕ. The results, shown in Fig. 3, are very satisfactory and form the basis for our assignment of *both* Γ_{15} and Γ_{25} modes as quasidegenerate at 26 meV. Comparison (Fig. 2) of the positions of the (522) and (600) peaks (the former is mostly Γ_{25}, the latter entirely Γ_{15}) suggests that Γ_{15} is marginally lower, but the difference in peak positions is considerably smaller than the instrumental resolution (~ 3 meV at $\Delta E \sim 30$ meV).

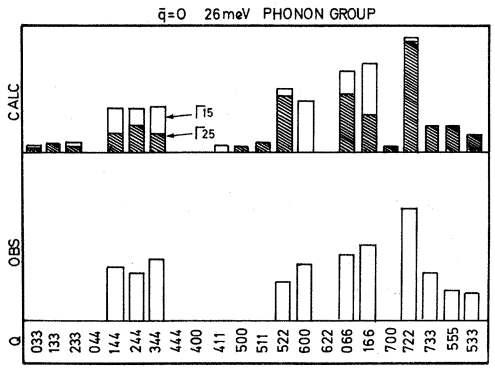

FIG. 3. Relative observed intensities of the 26-meV phonon group at various reciprocal-lattice points and calculated one-phonon scattering intensities assuming degenerate Γ_{25} and Γ_{15} modes. Two independent parameters (see text) were adjusted to produce the fit shown.

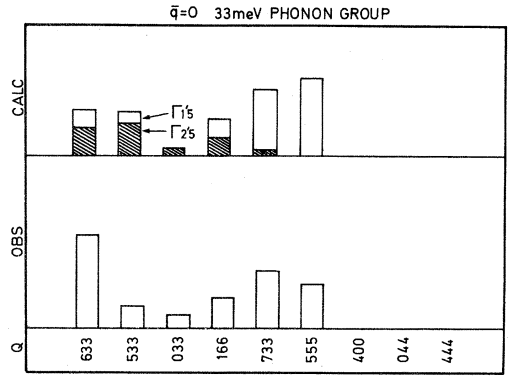

FIG. 4. Relative observed intensities of the 33-meV phonon group at various reciprocal-lattice points compared with one-phonon scattering intensities assuming degenerate Γ'_{25} and Γ'_{15} modes. There are no adjustable parameters.

Similar difficulties were encountered in explaining the intensities of the 33-meV $\vec{q}=0$ phonon group on the basis of a single (possibly degenerate) mode. Once again, the model calculations suggested a near degeneracy of the Γ'_{15} and Γ'_{25} modes and this assignment does indeed produce good intensity agreement (see Fig. 4). The problem here is a good deal less complex than for the Γ_{15}, Γ_{25} case as the eigenvectors are uniquely determined by symmetry. Consequently, less experimental data were necessary for its resolution.

Finally, Raman scattering studies[11] have placed the Γ'_{25} mode at 33.9 meV, in agreement with our assignment. The only other Raman-active mode, Γ_{12}, is observed to be at 37.7 meV in Cr_3Si.

IV. FORCE-CONSTANT MODEL AND DISCUSSION

We have already remarked that the results for a simple force-constant model influenced our interpretation of the data in initial stages, even though our analysis thus far is, in fact, model independent. Given the $\vec{q}=0$ mode assignments of Sec. III, there are a number of interesting questions for which even

a relatively simple Born—von Karman model may supply some answers:

(1) Can "reasonable" force constants account for the pattern of phonon frequencies summarized in Fig. 1?

(2) Can the model reproduce the $\vec{q}=0$ mode assignments, including the near degeneracies of the Γ_{15}, Γ_{25} modes and the Γ'_{15}, Γ'_{25} modes? If so, does the model suggest plausible physical explanations for these near degeneracies?

(3) Can the model reproduce the observed pattern of phonon intensities shown in Figs. 3 and 4, and thus verify the phonon eigenvectors which they imply?

The model which we have investigated contains only short-range forces between nearest-neighbor and next-nearest-neighbor chromium atoms, between nearest-neighbor Si atoms, and nearest Cr-Si neighbors. All interatomic potentials are assumed to be central, giving rise to radial and transverse force constants. There are thus eight force constants which can be adjusted. These force constants are identified in Fig. 5. This is a moderately large number of parameters, but not so large as to render a comparison with the observations meaningless. For example, we could use the observed $\vec{q}=0$ assigned mode frequencies to provide six constraints, and in principle the two mixing angles θ and ϕ provide two more constraints. The model then provides predictions for all the $\vec{q}\neq 0$ data, e.g., the entire behavior of the six observed acoustic branches. In practice, we chose instead to present another fit based upon a trial and error fitting of both the $\vec{q}=0$ modes and the limiting acoustic-mode velocities.

The resulting force constants are listed in Table II, and the calculated phonon dispersion along the three principal symmetry directions are shown in Fig. 1. The calculated phonon structure factors for the critical 26-meV phonon group are compared with observed values in Fig. 6. Considering the simplicity of the model (for example, screened Coulomb effects, known to be important in transition-metal lattice dynamics, are omitted), the fit is quite pleasing. We believe that the model parameters could serve as a basis for a more complete and microscopic calculation. The parameters seem plausible in a naive way, in that the longitudinal components are much greater than their transverse counterparts. The most interesting feature is the relative weakness of the near-neighbor (NN) chromium atoms, since the linear chain arrangement with its correspondingly small NN separation is one of the most distinctive features of the $A15$ structure. However, the phonon intensities calculated on the basis of the force-constant model (Fig. 6) are not as satisfactory as those calculated with purely phenomenological mixing angles (Fig. 3). This is particularly true for the (700), (733), (555), and (533) data. The measured intensities of the last three reciprocal-lattice points depend only on Si motion, and thus suggest that the Si eigenvectors given by the force-constant model may not be quite correct.

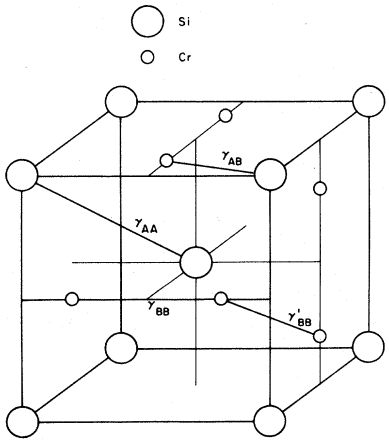

FIG. 5. Representation of the Cr_3Si structure showing the short-range force constants.

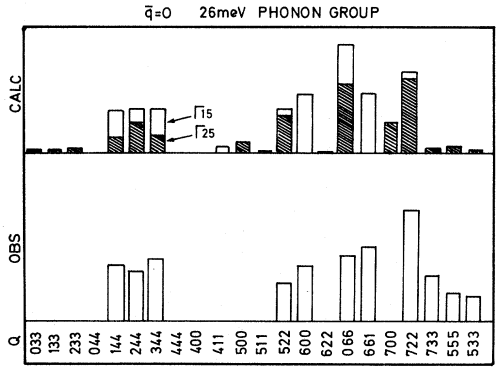

FIG. 6. Relative observed intensities of the 26-meV phonon group as in Fig. 3 compared with one-phonon structure factors based on Born—von Karman model calculations.

TABLE II. Born—von Karman force constants in units of 10^4 dyn/cm.

	Longitudinal	Transverse
Cr-Si	$\gamma_{AB}(l)=13.06$	$\gamma_{AB}(t)=-0.08$
NN Cr-Cr	$\gamma_{BB}(l)=4.30$	$\gamma_{BB}(t)=-0.13$
Si-Si	$\gamma_{AA}(l)=9.09$	$\gamma_{AA}(t)=0.00$
NNN Cr-Cr	$\gamma_{BB}(l)=0.46$	$\gamma'_{BB}(t)=-0.08$

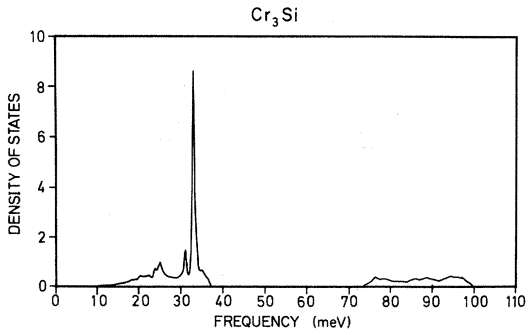

FIG. 7. Phonon density of states for Cr_3Si.

Having established affirmative answers to questions (1) and (3) above, it remains to comment upon the near degeneracies at $\vec{q}=0$ which complicated our analysis. An inspection of the Γ'_{15} and Γ'_{25} eigenvectors shows that they both consist of simultaneous displacements of Cr atoms on more than one chain transverse to the Cr-Cr chain directions. The Si sublattice does not participate. The differences are only due to the phases of the displacement waves on the chains. These mode frequencies are therefore identical in the absence of interchain coupling [$\gamma'_{BB}(l) = \gamma'_{BB}(t) = 0$, in our model]. Thus we see that the Γ'_{15}, Γ'_{25} near degeneracy is a consequence of the quasilinear aspect of the $A15$ structure, and may prove to be a general feature.

No such facile explanation of the Γ_{15}, Γ_{25} degeneracy presents itself. The fact that both the Cr and Si sublattices contribute to the eigenmodes means that, among other factors, the mode frequencies depend upon the ratio of the metal (Cr) and metalloid (Si) masses. However, repeating the above calculations for masses appropriate to Nb_3Sn rather than Cr_3Si showed the Γ_{15}, Γ_{25} near-degeneracy to be rather insensitive to this change in mass ratios. No deeper insight into this phenomenon can be given by us at this time, but we think it not unlikely that Nb_3Sn may, in fact, have near degeneracies similar to Cr_3Si.

Finally, we have used the force-constant model together with the parameters in Table II to evaluate phonon frequencies at arbitrary wave vectors and to integrate over the Brillouin zone (using the method of MacDonald *et al.*[12]) to generate the phonon density of states shown in Fig. 7. The sharp features of the density of states are readily correlated with dispersionless branches of Fig. 1 and no further discussion seems necessary.

Note added in proof. Another neutron study of phonons in Cr_3Si was just published by L. Weiss and A. Y. Rumyantsev, Phys. Status Solidi (b) 107, K75 (1981). Their results are less complete but in general agreement with those presented here.

ACKNOWLEDGMENTS

We wish to thank Robert Thomas for assisting with some of the critical checks of our data for spurious effects. One of us (J.-E. J.) has been supported by the Danish National Science Research Council and the W. C. Hamilton Fellowship Fund. We wish also to thank O. H. Nielsen for providing the computer codes for the density-of-states calculation. Work at Brookhaven National Laboratory was supported by the Division of Basic Energy Sciences, U. S. Department of Energy, under Contract No. DE-AC02-76CH00016.

*Permanent address: Kemisk Institute, Aarhus University, Aarhus, Denmark.

[1]For a recent review of lattice dynamics and superconductivity in $A15$ compounds, see P. B. Allen, in *Dynamical Properties of Solids,* edited by G. K. Horton and A. A. Maradudin (North-Holland, Amsterdam, 1980), pp. 97–196.

[2]G. Shirane and J. D. Axe, Phys. Rev. B 4, 2957 (1971).

[3]G. Shirane, J. D. Axe, and R. J. Birgeneau, Solid State Commun. 9, 397 (1971).

[4]B. P. Schweiss, B. Renker, E. Schneider, and W. Reichardt, in *Superconductivity in d- and f-band Metals* (Plenum, New York, 1976), p. 189.

[5]H. Wipf, M. V. Klein, B. S. Chandrasekhar, T. H. Geballe, and J. H. Wernick, Phys. Rev. Lett. 41, 1752 (1978).

[6]S. Schicktanz, R. Kaiser, E. Schneider, and W. Gläser, Phys. Rev. B 22, 2386 (1980).

[7]R. D. Blaugher, R. E. Hein, J. E. Cox, and R. M. Waterstrat, J. Low Temp. Phys. 1, 539 (1969).

[8]J.-E. Jørgensen, unpublished data.

[9]J.-E. Jørgensen and S. E. Rasmussen, J. Cryst. Growth 47, 124 (1979).

[10]B. N. N. Achar and G. R. Barsch, Phys. Status Solidi (b) 76, 577 (1976).

[11]S. B. Dierker, M. V. Klein, J.-E. Jørgensen, Z. Fisk, and G. Webb, Bull. Am. Phys. Soc. 26, 479 (1981).

[12]A. H. MacDonald, S. H. Vosko, and P. T. Coleridge, J. Phys. C 12, 2991 (1979).